International Journal of Hyperthermia

ISSN: 0265-6736 (Print) 1464-5157 (Online) Journal homepage: informahealthcare.com/journals/ihyt20

MicroPET-compatible, small animal hyperthermia ultrasound system (SAHUS) for sustainable, collimated and controlled hyperthermia of subcutaneously implanted tumours

A. K. Singh, E. G. Moros, P. Novak, W. Straube, A. Zeug, J. E. Locke & R. J. Myerson

To cite this article: A. K. Singh, E. G. Moros, P. Novak, W. Straube, A. Zeug, J. E. Locke & R. J. Myerson (2004) MicroPET-compatible, small animal hyperthermia ultrasound system (SAHUS) for sustainable, collimated and controlled hyperthermia of subcutaneously implanted tumours, International Journal of Hyperthermia, 20:1, 32-44, DOI: 10.1080/02656730310001609326

To link to this article: https://doi.org/10.1080/02656730310001609326

INT. J. HYPERTHERMIA
VOL. 20, NO. 1 (FEBRUARY 2004), pp. 32–44

Taylor & Francis
healthsciences

MicroPET-compatible, small animal hyperthermia ultrasound system (SAHUS) for sustainable, collimated and controlled hyperthermia of subcutaneously implanted tumours

A. K. SINGH, E. G. MOROS*, P. NOVAK, W. STRAUBE, A. ZEUG, J. E. LOCKE and R. J. MYERSON

Washington University School of Medicine, Department of Radiation Oncology, St Louis, MO 63108, USA

(*Received 14 February 2003; revised 16 May 2003; accepted 7 July 2003*)

An external ultrasound system was developed for the heating of subcutaneously implanted tumours in small animals. This small animal hyperthermia ultrasound system (SAHUS) was designed to be compatible with a microPET (small animal positron emission tomography) scanner to facilitate studies of hyperthermia effects on tumour hypoxia. Collimation and localization of energy deposition, a specific goal for the new device to avoid regional and/or systemic heating of small animals, was demonstrated using thermoradiography following high-power short-time heating of a layered gel phantom. The *in vivo* heating capabilities of the SAHUS were tested using PC3 cell line tumours (2000–2700 mm^3) grown in the lateral proximal thighs of Nu–/Nu– nuBR nude mice. Intratumour temperatures were recorded during heating trials with deep and superficial interstitial thermocouples. The experimental data showed that the SAHUS could produce hyperthermia in 8 ± 2 mm diameter tumours in small animals to a target temperature of 41.5°C and maintain it within a narrow temperature range (± 0.3°C) for up to 4 h without raising the core temperature of the animals. PET imaging studies, data to be published separately, were conducted before and during SAHUS-induced hyperthermia. Both devices performed as expected and there was no significant decrease in image quality. In this paper, the new SAHUS is described and data from phantom and *in vivo* experiments presented.

Key words: Animal, Cu(ATSM), hyperthermia, hypoxia, microPET, oxygenation, tumor, ultrasound.

1. Introduction

The re-oxygenating effect of hyperthermia has been demonstrated, but remains poorly understood[1–7]. Recently, there has been much interest in the relative radioresistance of hypoxic tumour cells. Copper-labelled diacetyl-bis(N^4-methylthiosemicarbazone) or simply ^{64}Cu(ATSM), has been shown to be selectively retained in hypoxic tissue[8–11]. We are studying the ability of localized hyperthermia to alter the oxygenation of subcutaneously implanted murine tumours using PET imaging with ^{64}Cu(ATSM).

To determine the minimum thermal dose to affect tumour oxygenation, a microPET-compatible hyperthermia applicator was needed to treat tumour-bearing mice. The first applicator was non-radiative and required the entire hind leg to be within a chamber filled with heat-conductive gel. The chamber was encircled with an elastic tubing coil through which heated water from a temperature-controlled water bath was circulated[12]. This system produced adequate heating of the tumour when properly controlled. However, maintenance of a steady gel temperature was difficult

*To whom correspondence should be addressed. e-mail: moros@radonc.wustl.edu

International Journal of Hyperthermia ISSN 0265–6736 print/ISSN 1464–5157 online
http://www.tandf.co.uk/journals
DOI: 10.1080/02656730310001609326

due to the long thermal response time characteristic of a conductive system. Consequently, maintenance of the tumour target temperature within a narrow range was extremely challenging. Simultaneous treatment of two mice was even more problematic. In addition, another significant disadvantage of this approach was that the entire submerged hind leg of the animal was also heated along with the tumour.

Moreover, it is known that different cellular effects predominate at different levels of hyperthermia[13]. Studies of thermal dose have shown that the effects of hyperthermia vary substantially with relatively small changes in temperature[13–16]. Consequently, the ability to produce and maintain hyperthermic temperatures within a narrow range was considered crucial to correlating time–temperature measures to treatment outcome in small animal experiments.

Adequate heating requires sufficient power deposition to achieve the target temperature. Subsequent temperature maintenance within a narrow range about the target temperature requires the ability to rapidly modulate power deposition within the tumour in response to changes in temperature. This can be achieved with a radiative device such as an ultrasound source. External heating of small tumours with ultrasound transducers, where power deposition is controlled by a temperature feedback loop, satisfies these requirements. Another advantage of ultrasound is the low potential for electromagnetic interference with other devices, such as a microPET, due to radiofrequency leakage[17]. Despite these advantages, an ultrasonic hyperthermia system for heating of animal tumours was last reported by Rivin *et al*. in 1980[18]. To the best of our knowledge, no ultrasound system for the heating of small animal tumours is presently available.

This paper describes a new ultrasound approach for the heating of subcutaneously implanted small animal tumours in more than one animal at the same time. Phantom and *in vivo* data indicate that this system provides localized, sustainable and controllable heating without any significant systemic heating.

2. Materials and methods

2.1. *Applicator design criteria*

The design for the applicator included the following criteria:

- Ability to heat small tumours implanted in mice's hind legs while maintaining internal tumour temperatures between 41 and 41.5°C for up to 60 min.
- Ability to deliver localized heating with minimum systemic effects.
- Ability to heat at least two mice simultaneously with adequate thermal control.
- Ability to fit inside the 12 cm diameter microPET bore (figure 1a) (Concorde Microsystems, Knoxville, TN, USA).
- Minimal perturbation of microPET (e.g. no fluid spills, no electromagnetic interference, no significant degradation of image quality).
- Easy access by radiological and animal personnel.
- Reusability.

The ultrasound system described below satisfied these criteria.

2.2. *Hyperthermia system design*

The physical configuration of the acrylic SAHUS applicator is shown in figure 1a with dimensions. Figure 1c shows how a small animal would be positioned so that a small tumour in its hind leg could be heated with the SAHUS.

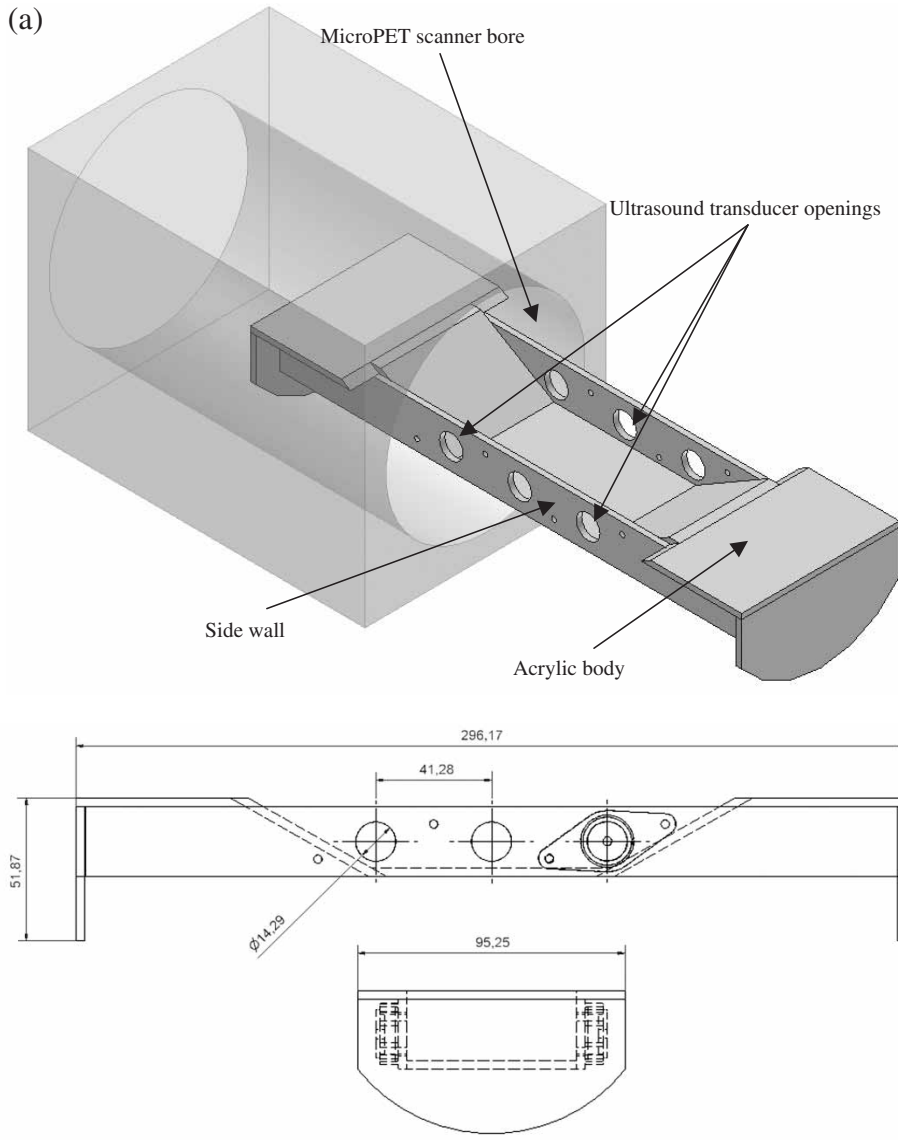

Figure 1a. Two-dimensional (2D) and 3D schematic diagrams of the SAHUS. The 3D image shows the applicator as it would fit within a 12 cm diameter cylinder that simulates the bore of the microPET scanner. The 2D diagram shows the main dimensions (mm) of the SAHUS.

The prime components of the entire SAHUS are shown in figure 2a. This system generates and controls the radiofrequency signals to drive piezoelectric element transducers (Lead Zirconate Titanate (PZT) – Navy Type I internal 'model' PKI-402, Piezo Kinetics, Inc., Bellefonte, PA, USA). Each transducer produced a collimated pressure field. Though there was some tumour-to-tumour variability, most heating was accomplished using about 10% (about 5 W) of the RF generator's maximum output capacity.

(b)

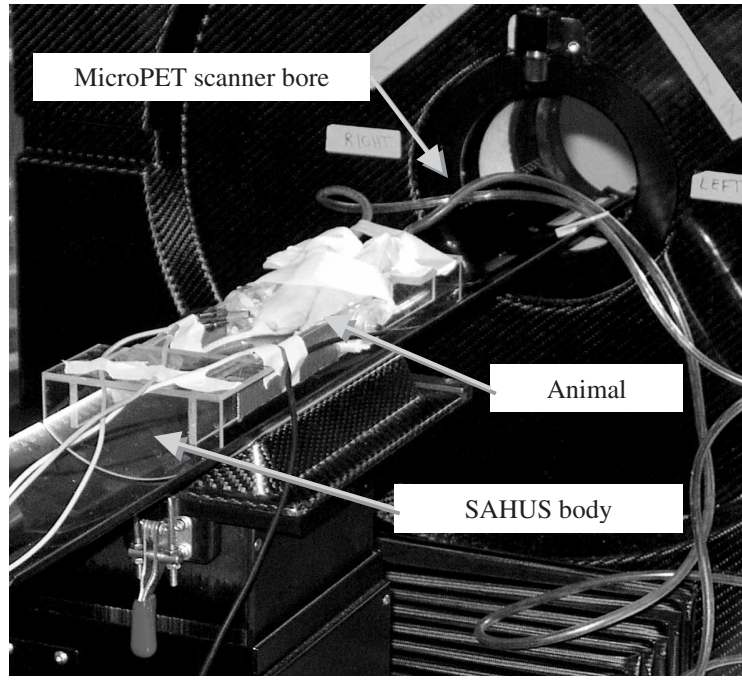

Figure 1b. Experimental setup for *in vivo* studies. The SAHUS with two mice is shown on the microPET tray.

(c)

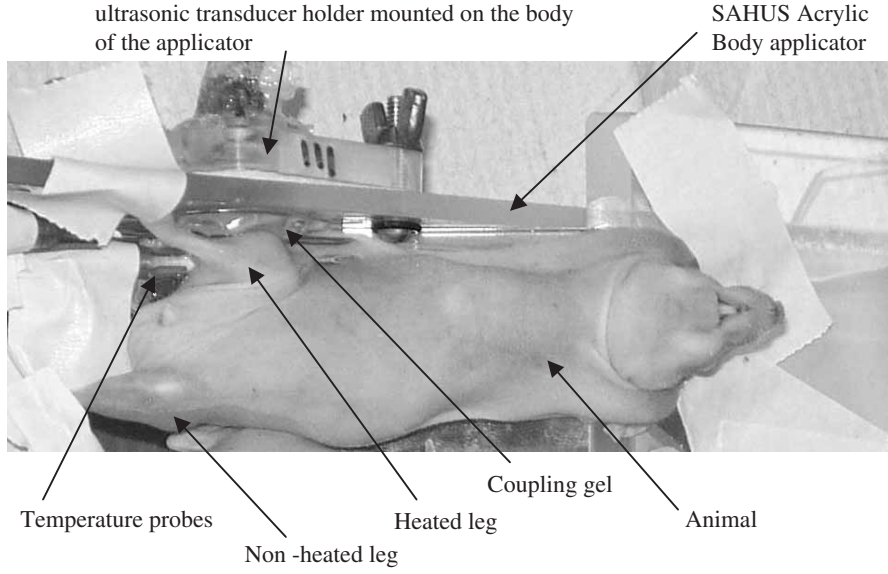

Figure 1c. Close-up view of the coupling between the tumour and the ultrasound source with acoustic gel. Temperature probes are shown in place.

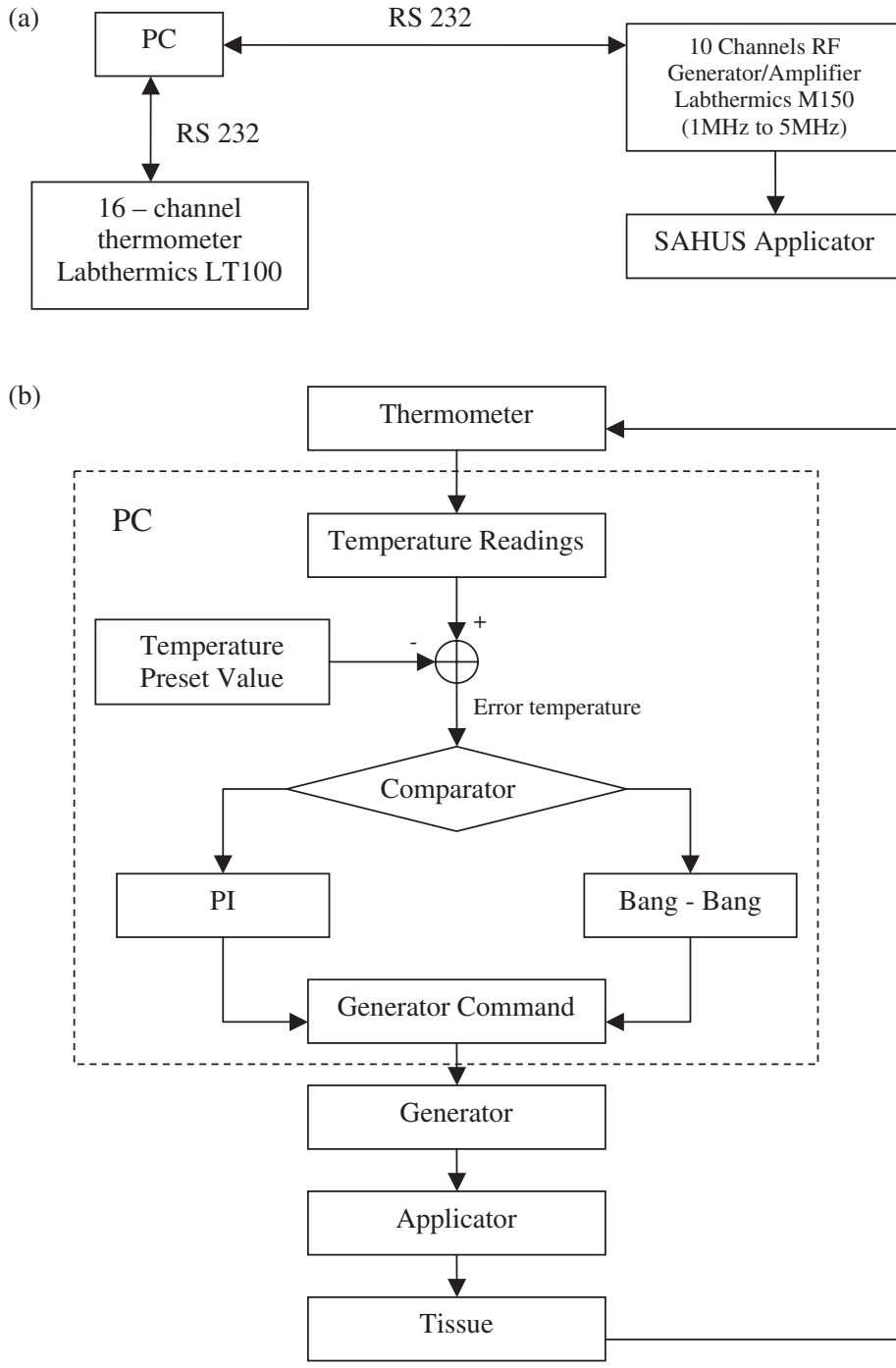

Figure 2. (a) SAHUS block diagram showing the main system components. (b) SAHUS control loop conceptual diagram.

2.2.1. *Thermometry*. Thermometry was performed with clinical-grade, 20-gauge copper-constantan needle thermocouples (Labthermics Technologies, Champagne, IL, USA). Within each needle was a single temperature sensor. These thermocouples were monitored with a 16-channel thermometry unit (Labthermics Technologies, Model LT-100). The measurement accuracy of this unit was 0.05°C at 25°C. Surface (tumour midline) and deep (distal margin) tumour measurements were taken. A single 16-gauge soft-plastic-coated thermocouple (Omega Engineering, Inc., Stamford, CT, USA) was used to obtain core rectal temperatures. There was no significant interference from the ultrasound-generating components of the system on any of the thermocouple readings.

2.2.2. *Temperature control*. Temperature data from the thermometry unit were sent directly to the controlling computer every 2 s. The radiofrequency (RF) generator (Labthermics Technologies, Model 150) had a maximum power output of 50 W per channel. The RF generator was linked via a serial RS-232 connection to a standard personal computer (Dell Optiplex GX240).

The PC-controlled the RF generator's power output for each channel with custom regulation software. For the experimental results presented in this paper, a feedback loop (figure 2b) was used with a proportional-integral plus bang-bang action (PIBB) temperature controller. This gave the SAHUS real-time temperature feedback control of power deposited in each tumour independently, thus, power deposition could be simultaneously controlled in more than one tumour at the time.

2.2.3. *PIBB control algorithm*. The PIBB algorithm functioned as follows. First a target temperature, T_t, and tolerance temperatures were defined. A relative tolerance temperature interval $\langle T_{\min}, T_{\max}\rangle$ was set as $\langle -3^{\circ}\mathrm{C}, +1^{\circ}\mathrm{C}\rangle$. Temperatures were read every 2 s. With each temperature reading, the maximum temperature measured in each animal was selected and then a weighted average temperature T_m of current and previous two measured-selected temperatures T_n, T_{n-1}, T_{n-2} was calculated and compared with the target temperature T_t. If T_m was below $T_t + T_{\min}$, the RF generator power was set to a predetermined and safe maximum value $P_{\max}$ (about 15 W). Note that $P_{\max}$ was not the maximum possible power that the system could achieve. If the measured temperature was above $T_t + T_{\max}$, the RF generator power was set to zero. If T_m was inside the interval $\langle T_t + T_{\min}, T_t + T_{\max}\rangle$, then the difference between T_m and the target temperature T_t was used for the calculation of a power change ΔP. The previous power value of the RF generator P_{prev} was adjusted by ΔP. This approach allowed the power level to remain near a constant value once steady-state was reached. Mathematically, the RF generator output power P_{out} for a given channel was calculated as follows:

$$P_{\text{out}} = \begin{cases} P_{\max}; & T_m < T_t + T_{\min} \\ 0 \le P_{\text{prev}} + \Delta P \le P_{\max}; & T_m \in \langle T_t + T_{\min}, T_t + T_{\max}\rangle \\ 0; & T_m > T_t + T_{\max} \end{cases},$$

$$\Delta P = 1.8 \cdot (T_t - T_m),$$

$$T_m = 0.5 \cdot T_n + 0.3 \cdot T_{n-1} + 0.2 \cdot T_{n-2}.$$

2.5. *Phantom studies*

As described by O'Neill *et al.*, a recipe based on polyacrylamide was used to make phantom material[19]. A block of the phantom was cut into 5-mm thick layers. A 21-mm diameter syringe was cut in half. The cylindrical portion of the syringe, with both ends opened, was used as a holder for the phantom layers. At the bottom of the cylinder, an acrylic slab was mounted to simulate the thickness and diameter of the opening for the ultrasound transducer (figure 1a). A holder with a 5 MHz transducer was mounted under the slab (figure 3). Up to four phantom layers, each 5 mm thick, were put into the cylinder and coupled with a 10 mm plug of standard ultrasound gel (Parker Laboratories, Aquasonic 100). The relative distances from the transducer to the phantom layers were chosen to mimic a typical *in vivo* situation for the SAHUS.

An infrared camera was positioned approximately 1 m above the upper end of the cylinder. As described by Chou and Moros *et al.*, infrared thermography was performed[20,21]. Thermographs of the phantom were taken with a Thermovision 480 IR Camera (Agema, Danderyd, Sweden). A baseline thermograph image of the upper phantom layer was taken first. Then, 15 W of net input power was applied for 15 s and another thermograph was taken of the phantom layer's surface.

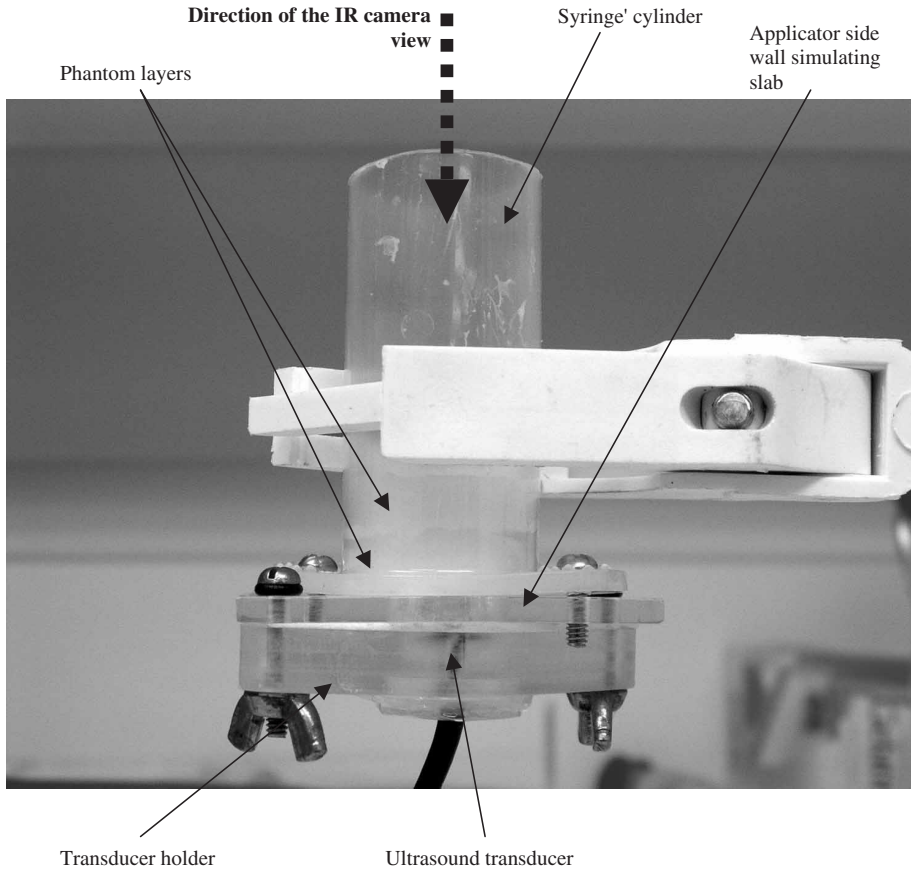

Figure 3. Phantom set-up for relative SAR measurements.

This measurement process was repeated with two, three and four (each 5 mm thick) phantom layers, which represented transversal cuts at distances of 15, 20, 25 and 30 mm from the surface of the ultrasound transducer, respectively.

Subtraction of the image taken immediately after heating from the preheating image, in each case, gave the distribution of surface temperature elevation produced by the forward and reflected ultrasound beam at the phantom–air interface. This distribution is directly proportional to the relative SAR distribution at planes parallel to the face of the transducer.

2.7. *Tumour model*

Tumours used to test the performance of the ultrasound device were PC3 cell line tumours implanted and grown in the lateral proximal thigh of Nu–/Nu– nuBR nude mice. These tumours were grown to be 8–10 mm in diameter.

2.8. In vivo *Experiments*

PC3 cells were used to grow tumours in the lateral proximal thigh of Nu–/Nu–nuBR nude mice. The tumours were grown to be 2000–2700 mm^3. The mice ranged in weight from 21 to 26 g and were anesthetized with an intraperitoneal injection of a ketamine and salazine solution dosed by weight (1 mg/kg). The anesthetized mice were positioned on the SAHUS tray and immobilized by taping their extremities to the tray. The hind leg tumours were positioned to abut the gel laden 5 MHz ultrasound transducers (figures 1b,c).

Two needle thermocouples were inserted into each tumour. One thermocouple was inserted near the surface (midline) of the tumour (in close proximity to the transducer) while the other thermocouple was positioned at the deepest portion of the tumour (closest to the femur and most distant from the transducer). A soft-plastic-coated thermocouple probe was introduced in the rectum to monitor core body temperature. Another probe was used to collect temperatures at several other locations in each mouse during experiments.

Once heating commenced, treatment control was completely transferred to the PC until it was time to end the treatment. The custom software allowed the operator to terminate easily treatment at any time. Temperatures were also recorded during the return to baseline tumour readings.

3. Results

3.1. *Phantom measurements*

Contour plots of relative SAR were generated from subtraction thermographs using a MATLAB program. Typical results are shown in figure 3. The patterns at various depths (distances from transducer face) clearly demonstrate the collimation of the ultrasound 5 MHz beam remaining within the projection of the 10 mm diameter transducer. Figure 3 also shows the expected narrowing of the beam's relative SAR with depth into the phantom due to ultrasonic attenuation. The plots were normalized to the global maximum value found in the layer at 15 mm from the transducer face (figure 4), which corresponds to a depth of 5 mm in phantom.

At 5 mm into the phantom, the 25% SAR contour covered the entire radiative projection area of the transducer. This is important because coverage of superficial tumours by the 25% iso-SAR contour has been correlated with long-term local control[22]. The pattern on figure 4b corresponds to the distal plane of a 10 mm diameter tumour.

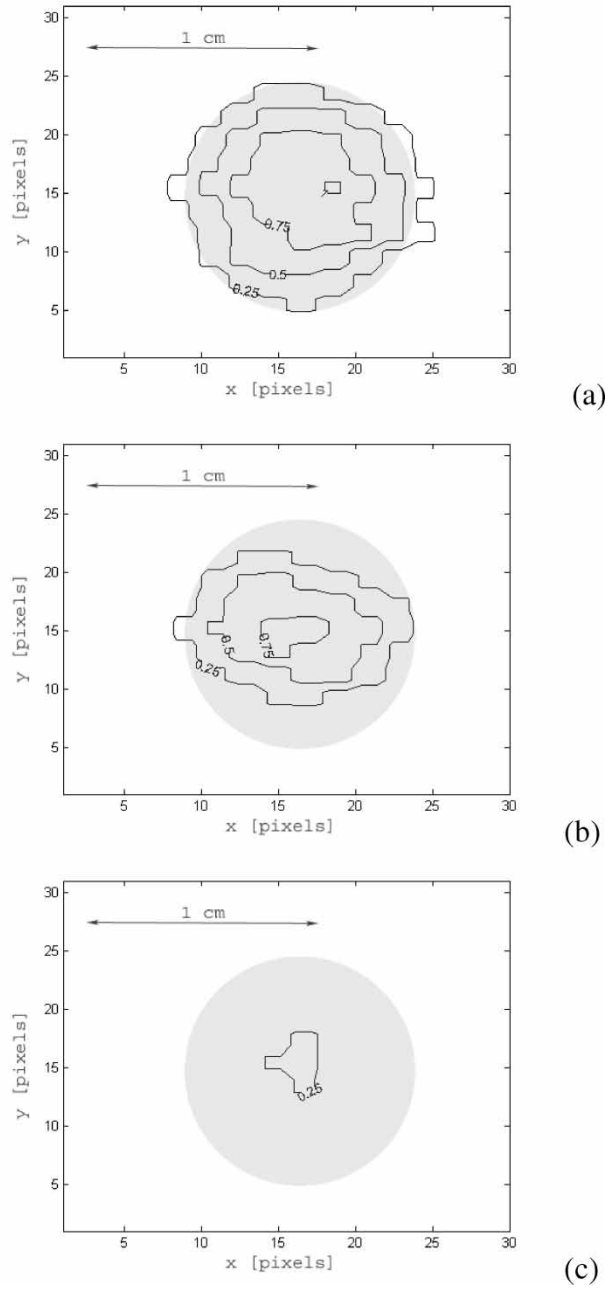

Figure 4. Relative iso-SAR contours in phantom from subtraction thermoradiographs using the SAHUS's 5 MHz ultrasound source as shown in figure 3. Plots a–c correspond to distances from the transducer of 15, 20 and 25 mm, respectively, since there was 10 mm of gel between the transducer face and phantom. These distances correspond to 5, 10 and 15 mm depths into phantom material. The 25% iso-SAR contour was not evident beyond 25 mm from the transducer. All images were normalized to the maximum value of the temperature raise found in (a) (about 6°C in this case). Transducer radiative area is marked by a gray circle. The distribution in (a) is representative of that present in the center plane of a 10 mm diameter tumour.

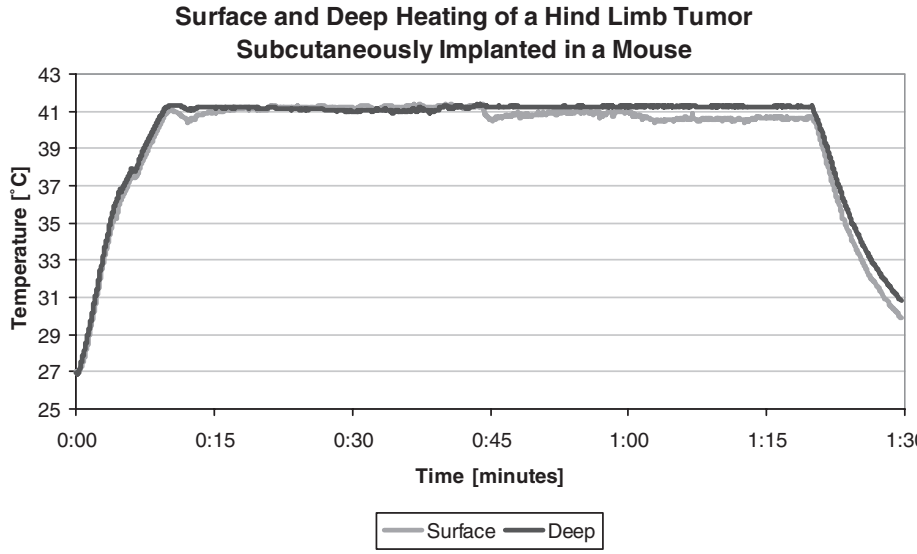

Figure 5. Time history of temperatures in two locations for a mouse heated in the SAHUS with a 5.0 MHz, 10-mm diameter ultrasound transducer. As shown, it took about 10 min to reach steady-state temperatures. Temperature control during the steady-state phase was within $\pm 0.3^{\circ}$C.

3.2. In vivo *experiments*

Two mice were successfully heated simultaneously as described in Section 2.6. Two piezoelectric element transducers were driven independently at 5.0 MHz. For both mice, there were no significant differences between the surface and deep tumour thermocouple readings. Representative temperature history results for one mouse are shown in figure 5.

No significant distant or systemic heating occurred as indicated by rectal thermocouples. During an experiment lasting 1 h, rectal temperature readings varied by a maximum of 0.6°C from baseline preheating values. During the same experiment, readings taken at the knee (just outside of the ultrasound field) showed less than 1.0°C variation from baseline.

3.3. *MicroPET compatibility*

One major concern regarding small animal hyperthermia studies was the possibility of water spills infiltrating and damaging the microPET scanner. Therefore, heating systems must be devised without open water. The first conductive device approach used a thermally conductive gel, but it still had water flowing in tubes and thus the possibility of water spills was not totally eliminated. The SAHUS design eliminated the use of water, thereby satisfying a major compatibility requirement.

Electromagnetic interference was assessed as outlined by Moros *et al.*[17] Briefly, the operation on the microPET and the SAHUS (including thermometry) was observed while both systems operated simultaneously and one at the time. No interference was detected. This observation was later confirmed when both systems performed as expected during animal experiments.

Degradation of image quality by the SAHUS was another major concern. Specifically, the main image-perturbing objects were the ultrasound transducers made of Lead Zirconate Titanate (PZT) – Navy Type I, a relatively high Z, ferroelectric polycrystalline ceramic material (Piezo Kinetics, PKI-402 material). Assuming that the 0.37-mm thick transducers were 100% lead, a worst-case scenario, a standard photon attenuation calculation revealed a photon fluence reduction of less than 6% for 511 keV photons[23]. In addition, in the final device, all metal parts (e.g. screws, bolts, etc.) were replaced with plastic parts.

Also, compatibility criteria restricted the size of the device so that it would fit inside the bore of the MicroPET while allowing easy access to laboratory personnel. Both criteria were easily met (figures 1a,b).

4. Discussion and conclusion

This paper presents an external ultrasound system for the heating of subcutaneously implanted small animal tumours. The goal of this project was to develop a system that could reliably deliver collimated-sustainable hyperthermia to an implanted tumour in a mouse model without limiting the ability to perform microPET scans.

Initially, there was concern that the piezoelectric element in this device would diminish the micro-PET image quality by photon attenuation. As demonstrated above, even assuming a worst-case scenario that the piezoelectric element had a Z equal to lead, there would still be 94% transmission of 511 keV photons. Experimentally, this amount of reduction did not affect image quality. Recent experiments within the microPET scanner have confirmed that the SAHUS meets the design criteria presented in Section 2, including good image quality. Detailed analysis of these and other imaging studies are beyond the scope of this paper and will be reported separately.

For sheer simplicity of use, the SAHUS is a marked advance from our original system, which heated the entire limb conductively. More importantly, the SAHUS is a marked advance because heating of an entire limb to heat a relatively small tumour necessarily caused changes in the perfusion of the entire limb. This change in limb perfusion confused interpretation of any measured changes in tumour perfusion or oxygenation. Thus, the SAHUS does a better job of mimicking clinical treatments on humans using planar superficial ultrasound systems and avoids the confounding effects of regional and/or systemic heating.

Moreover, with different sizes of piezoelectric element transducers and different tray configurations, a schematically similar ultrasound system can be adapted to treat a large range of tumour sizes in a variety of animal models as long as ultrasonic coupling can be assured. For instance, treatments combining heat with other agents such as radiation and chemotherapy can now be performed without inducing undesirable toxicity. Often hyperthermia of a limb tumour is achieved by placing the entire limb in a water bath[24]. This frequently results in necrosis of the footpad, a side-effect that does not reflect clinical conditions and may confound treatment results. Beyond confounding side-effects, animal studies that use such large region-heating schemes have attendant systemic effects. Such studies are unlikely to be reproduced in human patients because such systemic effects are very poorly tolerated[25–27].

Given the lack of confounding effects and ease of use, the SAHUS represents an advance in small animal hyperthermia technology. In addition to experiments

involving imaging studies such as microPET, a system such as the one described here has applications in multiple investigational settings.

Acknowledgements

Work was supported by NIH/NCI Grants R01 CA63121 and R01 CA71638.

References

1. Kim SH, Kim JH, Hahn EW. The radiosensitization of hypoxic tumour cells by hyperthermia. *Radiology* 1975; 114: 727–8.
2. Bicher HI. Increase in brain tissue oxygen availability induced by localized microwave hyperthermia. *Adv Exp Med Biol* 1977; 94: 347–51.
3. Morris CC, Field SB. Influence of hyperthermia on the oxygen enhancement ratio for x-rays, measured *in vivo*. *Br J Cancer* 1979; 40: 878–82.
4. Vaupel P, Otte J, Manz R. Changes in tumour oxygenation after localized microwave heating. *Prog Clin Biol Res* 1982; 107: 65–74.
5. Bicher HI, Mitagvaria NP, Bruley DF. Changes in tumour tissue oxygenation during microwave hyperthermia: clinical relevance. *Adv Exp Med Biol* 1984; 180: 901–5.
6. Song CW, Shakil A, Griffin RJ, Okajima K. Improvement of tumour oxygenation status by mild temperature hyperthermia alone or in combination with carbogen. *Semin Oncol* 1997; 24: 626–32.
7. Song CW, Park H, Griffin RJ. Improvement of tumour oxygenation by mild hyperthermia. *Radiat Res* 2001; 155: 515–28.
8. Fujibayashi Y, Cutler CS, Anderson CJ, McCarthy DW, Jones LA, Sharp T, Yonekura Y, Welch MJ. Comparative studies of Cu-64-ATSM and C-11-acetate in an acute myocardial infarction model: ex vivo imaging of hypoxia in rats. *Nucl Med Biol* 1999; 26: 117–21.
9. Obata A, Yoshimi E, Waki A, Lewis JS, Oyama N, Welch MJ, Saji H, Yonekura Y, Fujibayashi Y. Retention mechanism of hypoxia selective nuclear imaging/radiotherapeutic agent cu-diacetyl-bis(N4-methylthiosemicarbazone) (Cu-ATSM) in tumour cells. *Ann Nucl Med* 2001; 15: 499–504.
10. Lewis JS, Sharp TL, Laforest R, Fujibayashi Y, Welch MJ. Tumour uptake of copper-diacetyl-bis(N(4)-methylthiosemicarbazone): effect of changes in tissue oxygenation. *J Nucl Med* 2001; 42: 655–61.
11. Lewis JS, Herrero P, Sharp TL, Engelbach JA, Fujibayashi Y, Laforest R, Kovacs A, Gropler RJ, Welch MJ. Delineation of hypoxia in canine myocardium using PET and copper(II)-diacetyl-bis(N(4)-methylthiosemicarbazone). *J Nucl Med* 2002; 43: 1557–69.
12. Moros EG, Myerson RJ, Bigott HM, Sharp TL, Engelbach JM, Lewis JS, Laforest R, Kim J, McCarthy DW, Straube W, Welch MJ. A microPET-compatible heating applicator for tumour bearing mice to study the effect of mild hyperthermia on tumour oxygenation using 64Cu(ATSM) PET. Abstract presented at the 2001 Annual Meeting of the American Association of Physicists in Medicine, Salt Lake City, UT, July 25, no. 6782.
13. Sapareto SA, Hopwood LE, Dewey WC. Combined effects of X irradiation and hyperthermia on CHO cells for various temperatures and orders of application. *Radiat Res* 1978; 73: 221–33.
14. Leopold KA, Dewhirst MW, Samulski TV, Dodge RK, George SL, Blivin JL, Prosnitz LR, Oleson JR. Cumulative minutes with T90 greater than Tempindex is predictive of response of superficial malignancies to hyperthermia and radiation. *Int J Radiat Oncol Biol Phys* 1993; 25: 841–7.
15. Xia T, Sun Q, Shi X, Fan N, Hiraoka M. Relationship between thermal parameters and tumour response in hyperthermia combined with radiation therapy. *Int J Clin Oncol* 2001; 6: 138–42.
16. Dewhirst MW, Sim DA. The utility of thermal dose as a predictor of tumour and normal tissue responses to combined radiation and hyperthermia. *Cancer Res* 1984; 44(Suppl): 4772s–80s.
17. Moros EG, Straube WL, Klein EE, Maurath J, Myerson RJ. Clinical system for simultaneous external superficial microwave hyperthermia and cobalt-60 radiation. *Int J Hyperthermia* 1995; 11: 11–26.

18. Rivin BD, Longo FW, Tomashefsky P. Ultrasonic hyperthermia system for tumour irradiation. *Med Instrum* 1980; 14: 325–8.
19. O'Neill TP, Winkler AJ, Wu J. Ultrasound heating in a tissue-bone phantom. *Ultrasound Med Biol* 1994; 20: 579–88.
20. Chou CK. Use of heating rate and specific absorption rate in the hyperthermia clinic. *Int J Hyperthermia* 1990; 6: 367–70.
21. Moros EG, Straube WL, Myerson RJ. Potential for power deposition conformability using reflected-scanned planar ultrasound. *Int J Hyperthermia* 1996; 12: 723–36.
22. Myerson RJ, Emami BN, Perez CA, Straube W, Leybovich L, Von Gerichten D. Equilibrium temperature distributions in uniform phantoms for superficial microwave applicators: implications for temperature-based standards of applicator adequacy. *Int J Hyperthermia* 1992; 8: 11–21.
23. Kahn FM. *Physics of Radiation Therapy*. 2nd edn. Baltimore: Lippincott Williams & Wilkins, 1994, Appendix A-11.
24. Asea A, Mallick R, Lechpammer G, Ara BA, Teicher S, Fiorentino M, Stevenson A, Calderwood SK. Cyclooxygenase inhibitors are potent sensitizers of prostate tumours to hyperthermia and radiation. *Int J Hyperthermia* 2001; **17**: 401–414.
25. Perez CA, Scott C, Emami B, Hornback NB, Sneed PK, Asbell SO, Janjan NA. Evaluation of 45 degrees C hyperthermia and irradiation. II. A phase I clinical trial in humans by the Radiation Therapy Oncology Group. *Am J Clin Oncol* 1993; **16**: 477–81.
26. Van Rhoon GC, van der Zee J, Broekmeyer-Reurink MP, Visser AG, Reinhold HS. Radiofrequency capacitive heating of deep-seated tumours using pre-cooling of the subcutaneous tissues: results on thermometry in Dutch patients. *Int J Hyperthermia* 1992; 8: 843–54.
27. Van der Zee J, Hoff AM, Oudkerk M, de Kock W, van de Merwe SA, de Jong PC. Risk of acute hypotension following epidural analgesia during deep regional hyperthermia: a case report. *Int J Hyperthermia* 1992; 8: 625–9.